Near Surface Geophysics, 2015, **13**, 571-583 doi:10.3997/1873-0604.2015012

Investigating behind the lining of the Tunnel of Eupalinus in Samos (Greece) using ERT and GPR

Gregory N. Tsokas[1*], Jung-Ho Kim[2], Panagiotis I. Tsourlos[1], Georgios Angistalis[3], Georgios Vargemezis[1], Alexandros Stampolidis[1] and Nectaria Diamanti[1,4]

[1] *Exploration Geophysics Laboratory, Department of Geophysics, School of Geology, Aristotle University of Thessaloniki, 541 24 Thessaloniki, Greece*

[2] *Mineral Resources Research Division, Korea Institute of Geoscience and Mineral Resources, 92 Gwahang-no, Yuseong-gu, Daejeon 305-350, South Korea*

[3] *Egnatia Odos S.A., 6th km Thessaloniki–Thermi, P.O. Box 60030, 570 01 Thermi, Greece*

[4] *Sensors & Software Inc., 1040 Stacey Court, Mississauga, Ontario, L4W 2X8, Canada*

Received August 2014, revision accepted December 2014

ABSTRACT

The 2.5-km-long Eupalinian Aqueduct in the island of Samos, Greece, comprises the most impressive sample of ancient Greek engineering surviving almost intact. The main construction is a tunnel 1036 m long and almost 1.8 m wide excavated from both ends into mainly the massif limestone. In some parts of the overall length of about 240 m, the tunnel is dressed by lining of archaic and Roman age. This is of remarkable quality, and presumably, it protected the parts of the tunnel that were affected by subsidence and cave-ins. At some particular locations, it suffers deformations and other failures.

Thus, prior to its restoration and protection measures design, an integrated geophysical survey was carried out on the faces of the supporting walls, consisting in ground-penetrating radar and electrical resistivity tomography works. The survey aimed to investigate the structure at the unseen area behind the lining.

The thickness of the lining walls was accurately assessed by the ground-penetrating radar method and proved to be about 0.3 m–0.5 m on average. On the other hand, the width of the excavation behind the walls was predicted and checked at some particular locations with the electrical resistivity tomography works.

INTRODUCTION

The Eupalinian Aqueduct comprises a 2.5-km-long water feeding system built by ancient Greeks in the island of Samos (Greece). It consists of two pieces of duct enclosing the main construction, which is a 1036-m-long tunnel that was excavated from both ends by two simultaneously advancing groups. The way of designing and excavating comprises by itself an enormous achievement for the 6th century BC.

Not only visible failures of the lining of the tunnel but also partial collapses and cave-ins show that the rock mass suffers from instabilities, presumably caused by tectonic action. In this respect, the state-owned company "Egnatia Odos S.A." in cooperation with the Prefecture of Samos and the Ministry of Culture initiated a multidiscipline project aiming to protect and restore the monument. Therefore, a new surveying was initiated plus modern documentation like laser scanning and geological and geophysical investigations were carried out (Tsokas *et al*. 2014). These studies supported the geotechnical, structural, and architectural works which followed.

The integrated survey of Tsokas *et al*. (2014) assessed the present-day tectonic and geological setting above the northern and southern ends of the tunnel. It was a multidisciplinary approach employing very low-frequency, spontaneous potential, and seismic refraction; conventional resistivity tomographies (electrical resistivity tomographies (ERTs)); and finally a tunnel to surface electrical tomography. The result was that shear zones and faults were detected and the elastic moduli were assessed at some places.

The restoration of the failed sections of the lining comprised an essential part of the contemporary interventions described above. Consequently, its structure had to be investigated, and taking into account its unique historic and archaeological importance, the operation had to be fully non-destructive. In particular, the thickness of the lining had to be assessed and if possible to image the space behind its sidewalls. These tasks comprise the

* gtsokas@geo.auth.gr

aims of the integrated survey presented in these pages, which took place employing the methods of ground-penetrating radar (GPR) and ERT. Each one produced its own results, which combined to yield useful engineering information that supported the design of the intervention and restoration works of the project for the failed sections of the dressing of the walls.

The GPR method is evidently suitable for surveying against the walls of standing monuments (Linford 2004), and additionally, it is fully non-destructive. The method has been widely used not only in this respect but also for investigating beneath the floor of monuments (Indicative literature: Savvaidis *et al*. 1999; Leckebusch 2000; Colla and Maierhofer 2000; Piro, Goodman, and Nishimura 2003; Tsokas *et al*. 2007; Gaffney 2008).

Nowadays, the ERT can also provide images behind walls or beneath floors in a non-destructive manner. Copper flat base electrodes (Cosentino and Martorana 2001; Tsokas *et al*. 2008) can be employed for this purpose, as well as patches of bentonite mud (Athanasiou *et al*. 2007; Tsourlos and Tsokas 2007, 2011). Further, screw holders or medical electrodes were also applied for studying the moisture impregnation of historic walls (Colla and Maierhofer 2000; Sass and Viles 2006; Viles, Sass, and Mol 2008; Mol and Preston 2010). As an alternative to galvanic contacts, capacitively coupled electrodes could be used (Grard and Tabbagh 1991; Tabbagh, Hesse, and Grard 1993; Dabas *et al.* 1993; Dabas, Camerlynck, and Freixas I Camps 2000; Kuras *et al*. 2006).

THE EUPALINIAN AQUEDUCT

The most impressive ancient Greek technical construction that survived almost intact to our times is in the island of Samos in Greece. The 1.8-m-wide and 1036-m-long Tunnel of Eupalinos (pronounced Efpalinos in Greek) is part of the 2500-m-long Eupalinian Aqueduct used to channel the water from a point north of the ancient city of Samos into the walled urban complex.

The construction consists in a complex tunnel, dug into massive limestone and two ducts at either side; the northern one is about 895 m long and winds along the ravines of the mountain starting from the water spring of "Agiades" (Stamatakis 1990) to the northern portal. This construction is entirely out of the ancient city walls. Respectively, at the southern portal, a 620-m-long subterranean duct brings the water to the fountains in the ancient city. The southern entrance lies in the walled part of the city.

FIGURE 1
View of the Eupalinian Tunnel at the point where a Byzantine chapel was made at AD 500–900.

According to Herodotus, the whole construction was designed and realized by engineer Eupalinos, son of Naustrophus from Megara, some time during the 6th century BC. The tunnel was excavated from both ends having a meeting point at about the centre, and the measured mismatch (Kienast 1995) is very small even to the present-day standards. Nowadays it is clear that a geometry-based sophisticated approach was employed by Efpalinos to keep the tunnel aligned and to ensure that the two opposite advancing groups will meet under about 160 m of solid rock (Goodfield and Toulmin 1965; Van der Waerden 1968; Burns 1971; Kienast 1995; Frumkin and Shimron 2006; Stiros 2009).

This aqueduct system was used for about a thousand years, as proved from archaeological findings. A small chapel near the centre, which is Byzantine, dated to about AD 500–900 (Fig. 1), proves that people have entered it during that time (Apostol 2004). It was rediscovered in 1853 by French archaeologist Victor Guérin (1856).

The tunnel was cleaned and studied systematically by Kienast (1995, 2005). Today, about 100 m of the main tunnel starting from the south entrance is accessible to the public. In fact, among others, the study to be presented in these pages was performed in order to aid the restoration workings that will make the full length of the tunnel accessible.

The cistern, which is under a medieval church (Fig. 2), was used to collect water. From that point, the water was driven in the underground duct with a slope of 0.20% up to the northern portal of the tunnel (Kienast 1995; Psilovikos *et al.* 2003). The northern duct was constructed employing the "cut and cover" technique.

The main tunnel is dug into the massive limestone mainly (Fig. 2). The floor is at about 55.5 m above the sea level. The rock mass overlaying the tunnel is 175 m thick at the most under the top of "Ampelos" Hill.

A 0.60-m-wide trench was dug at the west side or directly beneath the tunnel. This is 3.8 m deep at the north portal reaching 8.9 m at the southern one (slope 0.36%). The water supply was made by open-topped clay pipes (gutters), which were put at the bottom of the trench. The trench was bridged by stone slabs, and it was partially refilled by the debris of the digging. The spread of this type of underground construction in the Greek world proves that the relevant techniques were well known (Doerpfeld 1894). Consequently, we have essentially two tunnels, the upper wider one, which even nowadays can be walked through, and the lower narrow one, which has been cleaned in its major part. A photograph of the upper tunnel is also shown in Fig. 3.

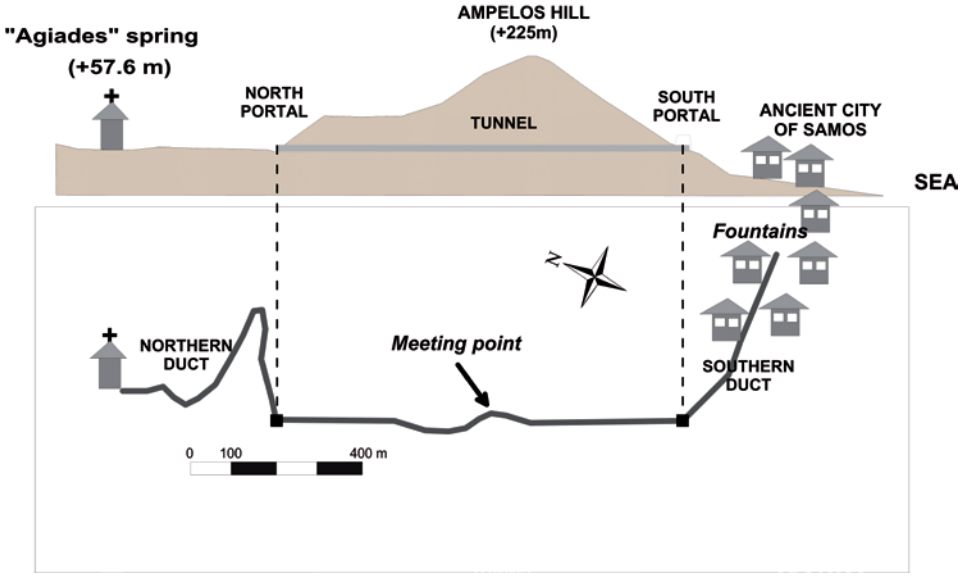

FIGURE 2
Drawing of the side (up) and plane view (down) of the Eupalinian Aqueduct. The main construction was a complex tunnel through the mountain, made by drilling the massive limestone simultaneously from both ends. This is depicted by the grey straight line on the side view (upper part), whereas its plane view shows various deviations from the straight line. Two buried ducts are connecting the ends to the springs and fountains, north and south of the tunnel, respectively. As seen at the plane view (lower part of the figure), the northern duct winds along the ravines until it reaches the northern portal.

A shallow buried channel similar to the northern one was made to lead the water from the southern exit to the fountains of the ancient city (eastwards of the southern end). The length of this urban conduit is about 620 m and slopes at about 0.75%.

The tunnel is dressed by stone or brick masonry to a cumulative length of about 240 m. Most of this lining was made at the Archaic era, whereas a much smaller portion was built during the Roman times. This ancient lining is of excellent quality, but nowadays, it suffers at several locations by stress-induced damages. These are evidences of instabilities of rock mass rendering necessary geotechnical measures that will guarantee the safety of the visitors in the future.

TOMOGRAPHIES ON THE WALL OF THE TUNNEL

A number of tomographies were carried out on the sidewalls of the stone masonry lining of the tunnel. The aim was not only to image, as much as possible, the invisible area behind the face of the lining but also to penetrate even deeper in order to gain information that could help in assessing the quality and the moisture content of the rock mass.

A distance-measuring system along the tunnel had been established by Kienast (1995). The starting point was set at the northern portal, and tagged nails were put every 10 m. We used this system as reference, but our work was also geo-referenced to the Greek National Grid. Hence, the abbreviation "LDMS" will be used hereinafter standing for local distance-measuring system.

Each tomography that was conducted against the wall started from a particular point along the LDMS. In order to find a convenient and comprehensive way of referring to various ERTs, we decided to include the starting distance in the respective code name. Additionally, each name contains two indices; the first shows whether the tomography was carried out on the east or the west sidewall, whereas the second states the height above the tunnel's floor where the tomographic line was placed. If the line was put at the height of 110 cm, the index is UP, whereas it is DOWN if the height was 60 cm. In other words, two transects were established at two distinct heights. For example, the name ER_20_DD_EAST_UP means that the tomography started at the 20-m tag of the LDMS, the dipole–dipole array was employed, and it was conducted on the east sidewall 1.10 m above the floor.

FIGURE 3
View of the start of the archaic lining from an undressed portion of the tunnel.

The approach of measuring at two heights was imposed by the particular geometry of the tunnel. The initial schedule was to carry out just one tomography at about the centre of the lining wall, but finally, we ended out that we would have better control with two parallel tomographies. These had to be carried out at the heights referred; otherwise, one would have to be very close to the floor and the other very close to the arched roof.

FIGURE 4
The measuring tape is 1.10 m above the floor of the tunnel and marks one of the ERT profiles carried out. The bentonite patches on both walls comprise the non-invasive electrodes used, whereas the bunch of cables connecting the electrodes to the multiplexer of the instrument is also seen.

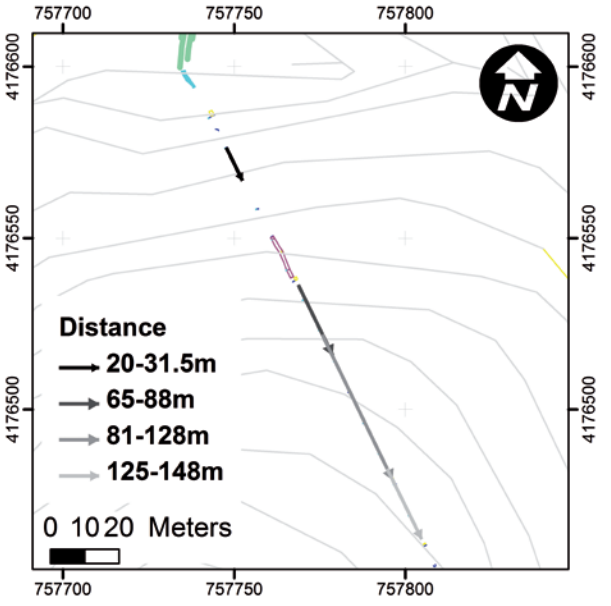

FIGURE 5
All ERTs that were conducted on the faces of the lining in the northern end of the Eupalinian Tunnel.

Several factors were taken into account for designing the survey, i.e., for selecting the suitable array, the interprobe spacing, the length of the dipoles, etc. This "parameter setting" procedure was aided by the rough knowledge about the possible thickness of the lining and also of the width of the excavation behind it (Angistalis *et al*. 2014). We also knew that the area behind the dry masonry of the archaic lining up to the excavation perimeter is backfilled with well-stacked partially worked stones. However, the existence of carved areas, subsidences, and spots of rock failures was expected to be concealed behind the lining. All the aforementioned factors indicate that a strongly lateral resistivity variation was much likely to exist.

However, the face of the dressing was fairly flat, a fact that facilitated the conduct of the survey. Further, the bentonite mud patches were easily stuck on the stone masonry (Fig. 4), which retained a lot of moisture to guarantee excellent electrical coupling. The plasticine-like wet bentonite patches (Athanasiou *et al*. 2007; Tsourlos and Tsokas 2007, 2011) were easily stuck on the faces of the lining and also easily removed afterwards. In fact, after the patch was taken out, the wall was rubbed by a wet sponge to disappear the residual traces of the stacked material.

The aforementioned factors led us to the selection of the dipole–dipole array and the following data acquisition parameters.

- The interprobe spacing (a) was set to 1 m except for one tomography (ER_20_DD_EAST_UP), which was carried out with a = 0.5 m.
- The current to potential dipole distance (nXa) had its maximum value for n = 8.
- After completing the sequence of readings for the initial spacing "a", the last was doubled ($2a$) and an additional sequence was measured.
- Finally, the spacing was tripled, and measurements were taken once more.

An IRIS SYSCAL-PRO resistivity meter was used, which is capable of ten simultaneous potential readings. All other gear was custom built, including the multi-clone cable of 48 exits.

Figure 5 shows the direction and length of all tomographies carried out on the walls of the tunnel. After the data collection in the manner described earlier, they were cleaned of extreme erratic readings and subjected to inversion along the base lines described by Tsourlos (1995) who also produced the relevant software. This algorithm performs iterative smoothness constrained inversion (Constable, Parker, and Constable 1991), employing a 2.5-D finite-element forward solver. All tomographic images produced show a low misfit error between the real and the calculated data (3%), which is indicative of the good data quality.

Figure 6 shows the electrical tomography carried out on the west wall of the lining, 1.1 m above the floor, between the LDMS positions 65 and 88. It reveals a stratum of high resistivities that starts at the face of the lining, but its ending surface seems to undulate about a plane 1 m away from the face. After this relatively antistatic material, a conductive one appears that contains parts where the resistivity is between 15 Ωm and 30 Ωm. Seeking an interpretation for the tomographic image, we compared the findings with a sketch of the cross section of the tunnel at the position 0+63.9 (LDMS), as shown in Fig. 7. The comparison shows that the undulating back surface of the resistive material corresponds to the interface between the backfill behind the lining and surrounding ground. In other words, the material of relative lower resistivity behind this interface is attributed to the rock mass. As noticed before, some areas of much lower resistivity (15 Ωm–30 Ωm) do exist in this formation. Therefore,

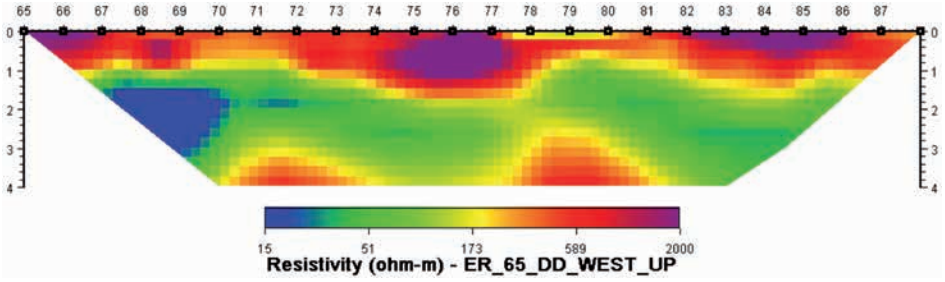

FIGURE 6
Result of the inversion of the data for the tomography ER_65_DD_WEST_UP.

they should be areas of high water content that confronts to the observed points of water dripping (blue circle in Fig. 7).

Two tomographies were carried out in the interval between the 81st m and the 128th m of the LDMS, each on every side of the tunnel at the height of 1.1 m above the floor. The archaic masonry dresses the walls in this area. The images obtained (ER_81DD_EAST _UP and ER_81DD_WEST _UP) are shown in Fig. 8.

Both tomograms of Fig. 8 clearly show the undulations of the rims of the excavated area, which are unseen behind the lining. The area between the lining and these limits of the excavation is filled presumably with the same staff as has been revealed elsewhere, i.e., with well-stacked partially worked stones mainly coming from the debris of the original excavation. The low-resistivity areas, which are depicted with cold colours and, in particular, the blue ones, presumably reflect the presence of zones with increased moisture content.

At the distance of 0+100 m (LDMS), a significant deformation of the tunnel is observed, witnessing the imposition of severe stresses. In fact, when the archaeological investigations and cleaning were taken place, the west wall was partially reconstructed using brick mortared masonry. Obviously, this procedure was a first-class opportunity to see the structure of the lining and the quality of the backfill (Jantzen *et al*. 1973; Kienast 1995). As far as the present study is concerned, Kienast (1995) reported that the space behind the lining up to the excavation front is backfilled by well-stacked partially worked stones. It was also verified that this material fills also the space behind the arched stones of the roof. The backfill minimizes the potential thread for ground collapses behind the lining. Figure 9 shows a comparison of the actual measured thickness of the backfill with that predicted using the ERT method. The tunnel's cross section has been drawn at the LDMS point 0+100 m. Clearly there is good correspondence between the high–low-resistivity interface and the backfill–rock front.

Angistalis *et al*. (2014) have shown other examples of comparison of the geophysical images with the archaeological findings, which confirm one by one that the hypothesis established. That is, the undulations of the low-resistivity material, which is depicted in the ERT images, correspond with the undulations of the surface of the rock mass.

Four tomographies were carried out between the LDMS positions 125 m and 148 m, one pair at each side. That is, ERTs were conducted at the DOWN (at 0.60 m above the floor) and UP (at 1.10 m) modes. The inverted resistivity distributions are shown in Fig. 10. It is shown that the eastern side, for both levels, shows

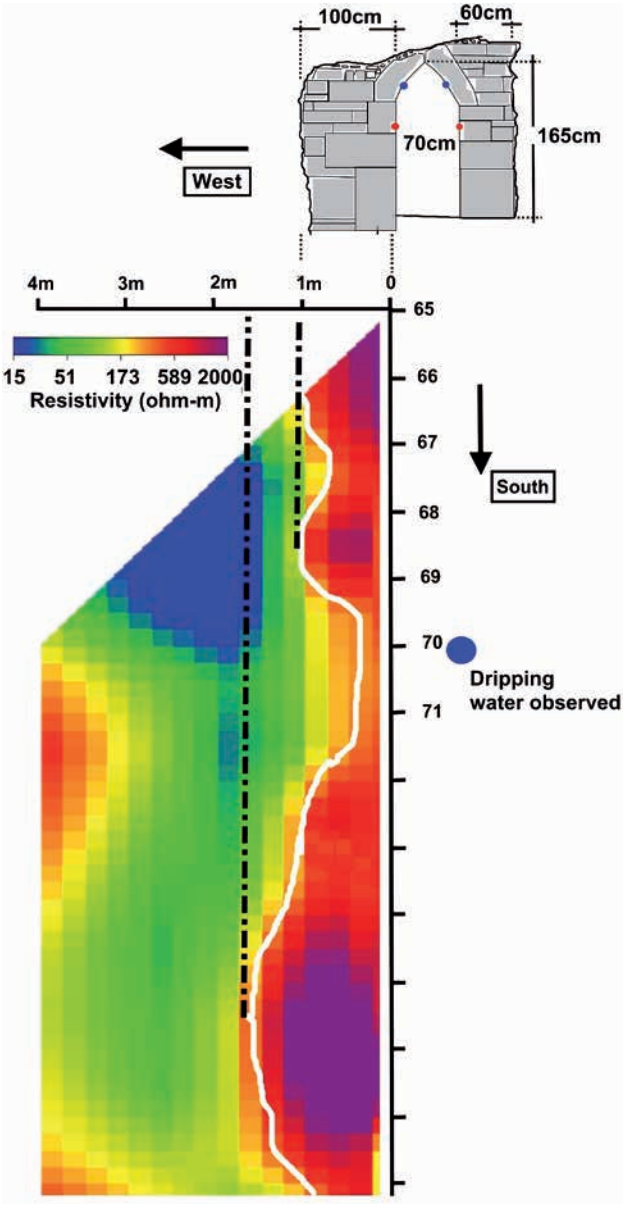

FIGURE 7
The findings on the tomography ER_65_DD_WEST_UP are compared with a cross section of the tunnel and the lining at 0+63.9 of the LDMS. The blue and red dots on the cross-sectional sketch depict the ERT sections carried out at two elevations and perpendicular to the drawing.

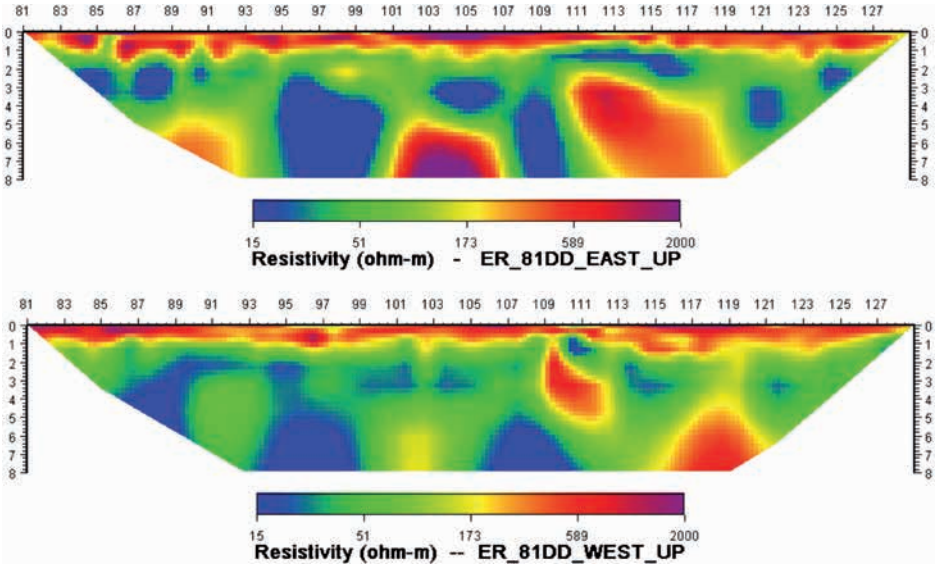

FIGURE 8
The upper part shows the tomography ER_81_DD_EAST _UP while ER_81_DD_WEST _UP is at the lower.

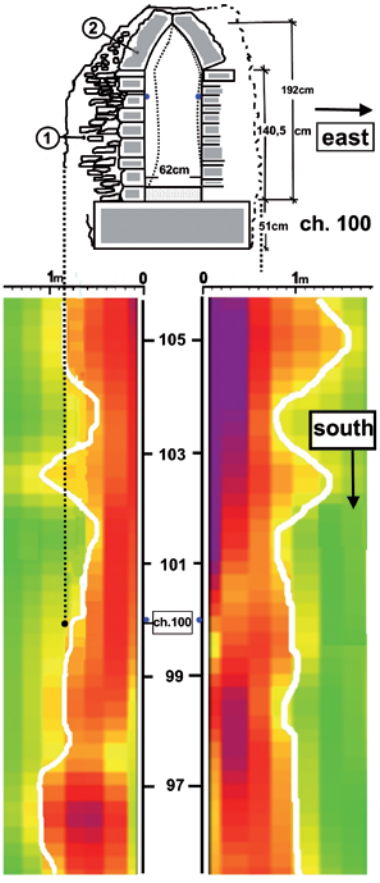

FIGURE 9
Parts of the tomographic images of ER_81_DD_EAST _UP and ER_81_DD_WEST _UP about the LDMS location 0+100. A sketch of the tunnel's cross section is also shown, which was drawn after the extraction of the lining's stones during the restoration workings (Jantzen *et al*. 1973). 1: Well-structured backfill. 2: Hewn stones of the lining walls.

increased moisture at the positions 131 m–134 m, 138 m–140 m, and 144 m–146 m. Respectively, the western side shows increased moisture in the interval 127 m–140 m. The difference in relative wet areas of the rock mass between the two sides may be attributed to possible direction of water flow from east to west.

Continuing the working hypothesis about the clear imaging of the excavation front on the ERT results, we can relative safely say that at the 1.10-m level, the excavation width reaches the maximum value of about 2 m at either side. However, at the 0.60-m level, the width reduces to less that 1 m at some particular locations. This is attributed to cave-ins that affected both sidewalls during the initial tunnel excavation (Angistalis *et al*. 2014).

The excavation surface seems to undulate, but it has an unusual recess at the western side at the positions between 143 m and 145 m at the level of 1.10 m above the floor. Another possible recess may be inferred from the pattern of the resistivity anomaly between 138 m and 141 m shown at the profile ER_125_DD_EAST_DOWN (Fig. 10B). If this interpretation will be proved correct in the future, then it is much likely that the south wall of the recess is sharp.

HIGH-RESOLUTION ERT BETWEEN THE POSITIONS 0+20.00 M AND 0+31.50 M

The tomography that had the code ER_20_DD_EAST_UP was carried out on the east face of the lining among the LDMS positions 0+20.00 m and 0+31.50 m at the level of 1.10 m from the tunnel's floor. In contradiction to the rule followed for the interprobe spacing of all other tomographies, this distance was set to 0.50 m for this particular one. The inverted data resulted in the image in Fig. 11.

Since the spacing was small, the result reveals a thin resistive layer at the surface of the wall attributed to the thickness of the lining itself, whereas a relatively more conductive layer is hidden behind believed to represent the backfill material. This layer is

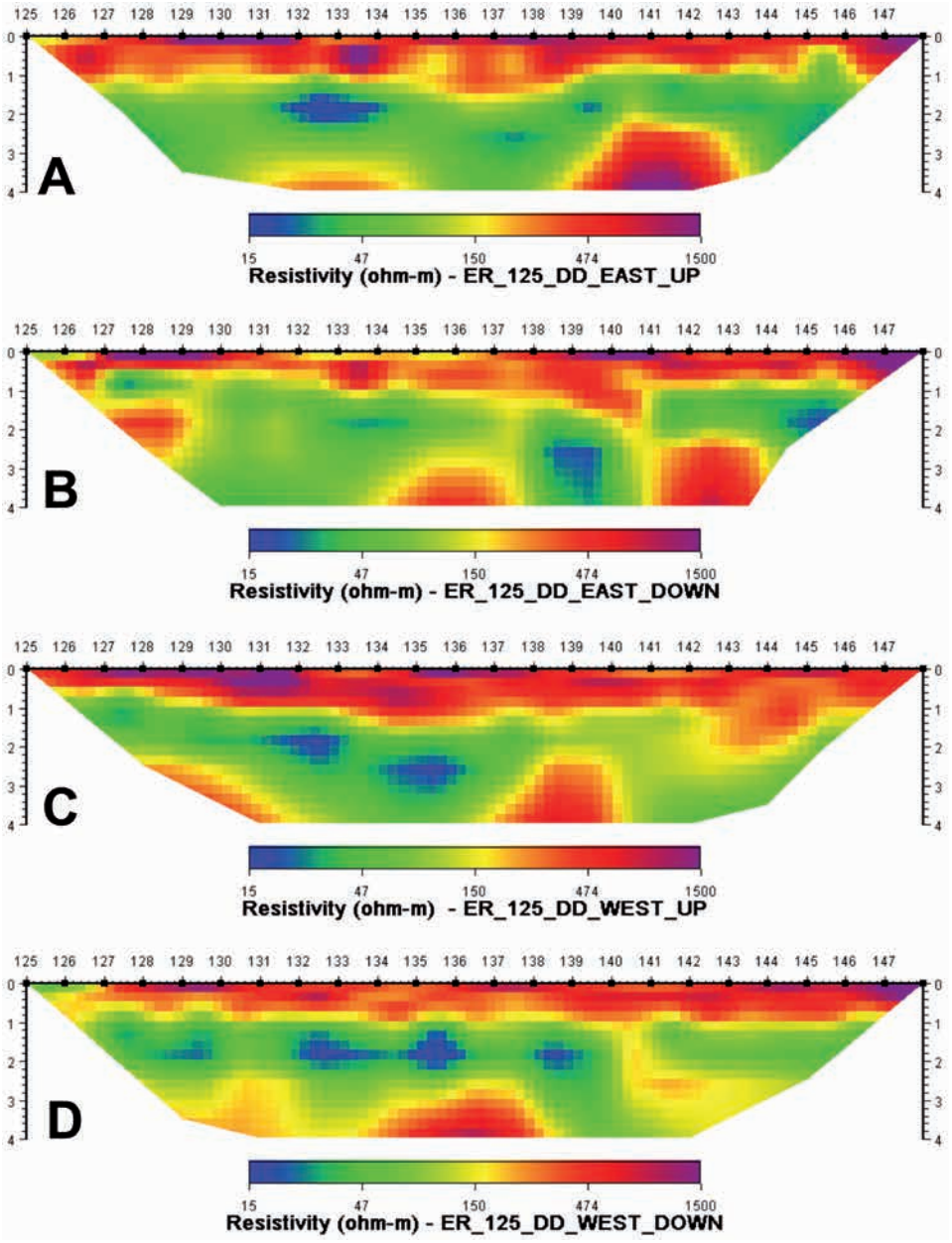

FIGURE 10
The tomographies carried out between the positions 0+125 m and 0+148 m. The annotation UP refers to the level of 1.10 m above the floor, whereas DOWN refers to the level of 0.60 m. The tomographies on the east wall are in A and B, whereas those on the west wall are in C and D.

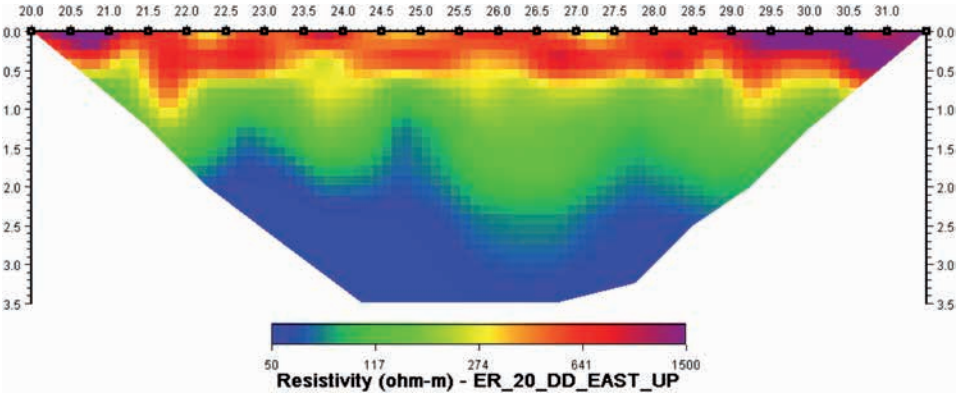

FIGURE 11
The tomography ER_20_DD_EAST_UP that was carried out with 0.5 interprobe spacing. Thus it is of higher resolution than all the others conducted on the walls of the lining of the Eupalinian Tunnel.

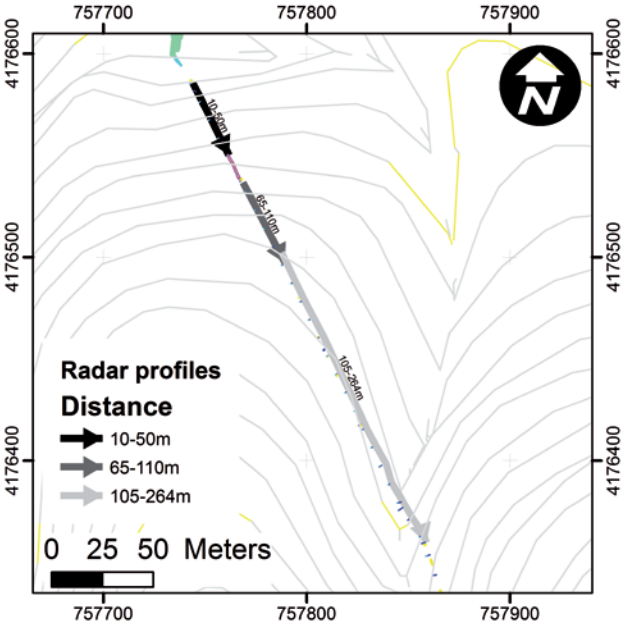

FIGURE 12
Sketch map of all transcripts that was carried out against the lining at the northern end and of the Eupalinian Tunnel, at both sides. The drawing was also referenced in the National Greek Grid.

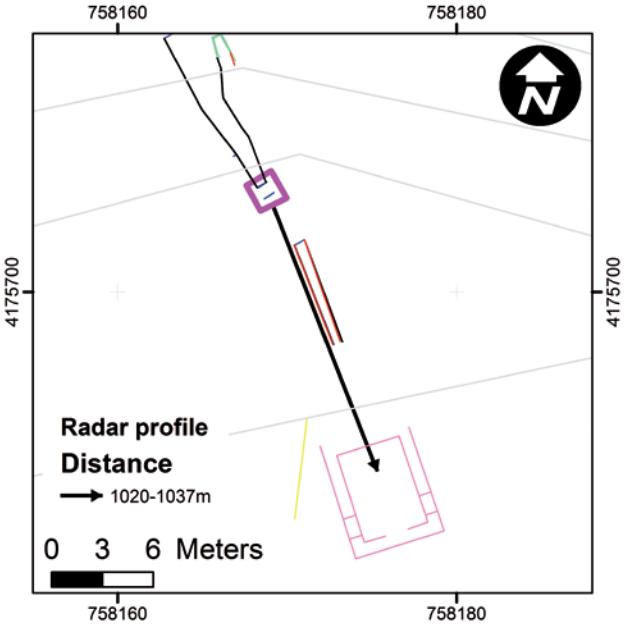

FIGURE 13
The transects that were carried out against the east and west walls at the southern portal of the Eupalinian Tunnel. The drawing was referenced in the National Greek Grid.

followed by an even more conductive layer that is the more distant one from the face of the lining. The latter is interpreted as the rock mass.

The smaller spacing renders this tomography as a higher resolution one and therefore as the most compatible with the radar results that will be presented in the next paragraph. The thickness of the lining is found to be about 0.40 m–0.50 m, whereas the excavation front is relatively far behind the lining face, at about 1.5-m depth.

GPR INVESTIGATIONS BEHIND THE LINING'S FACE

The structure of the lining was further investigated employing the GPR method, which is, in principle, of much higher resolution than the ERT. A number of GPR profiles were carried out constituting a total length of 772 m. Their location is shown in Figs 12 and 13, respectively, for the northern and southern ends of the tunnel. The codified names used follow the same convention for the ERTs. That is, for each GPR transect, the starting position in the LDMS comprises part of the codified name and the flags EAST and WEST to state on which wall it was carried out. Additionally, the flags UP and DOWN state whether the profile was located far or close to the floor, respectively. This distance from the floor varied for different profiles. Also, some of them were carried out on the faces of the arched roof though generally it was impossible to move the antennae there because of the limited space, as a result of the deformation and other damages. Emphasis was put on the positions where failures of the lining had been observed and mapped (Zambas 2009).

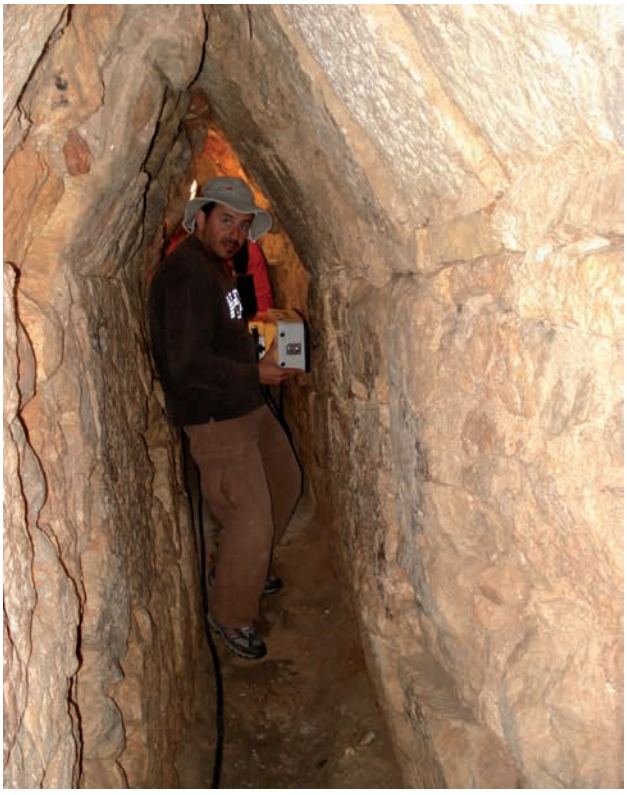

FIGURE 14
Collection of GPR data along a profile established on the wall dressing the excavation of the Eupalinian Tunnel.

The 800-MHz ABEM RAMAC antennae of MALA were used, and spacing between successive traces was set to 0.05 m. Data were subjected to the removal of the DC component and band-pass spatial filtering with cut-off wavelengths of 0.05 m and 15 m. Next, they were amplified, employing exponential function, and undergone temporal filtering (lower threshold at 101 MHz and ramp up to 202 MHz, start of upper ramp at 1400 MHz and threshold at 1800 MHz). Finally, normal-move-out correction was applied to all data.

The 450-MHz PULSE EKKO antennae were used in common

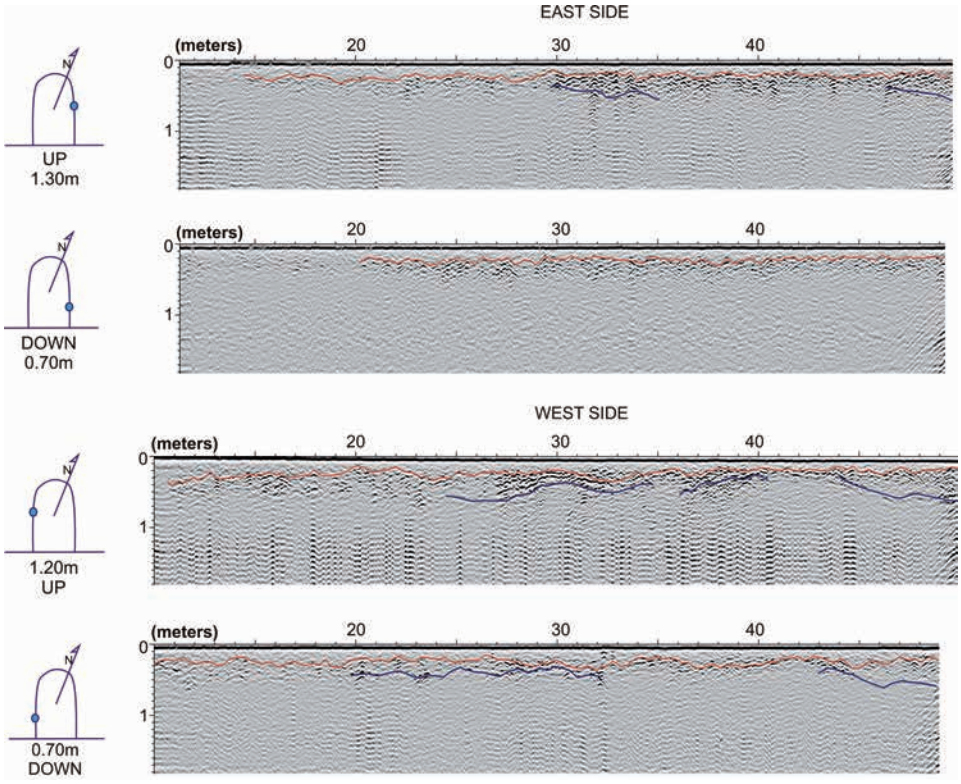

FIGURE 15
Processed GPR sections on the sidewalls of the lining of Roman age between the LDMS positions 0+10.0 m and 0+50.0 m. The small sketches on the left depict the direction of the profiles, whereas the dots mark the levels where they were carried out.

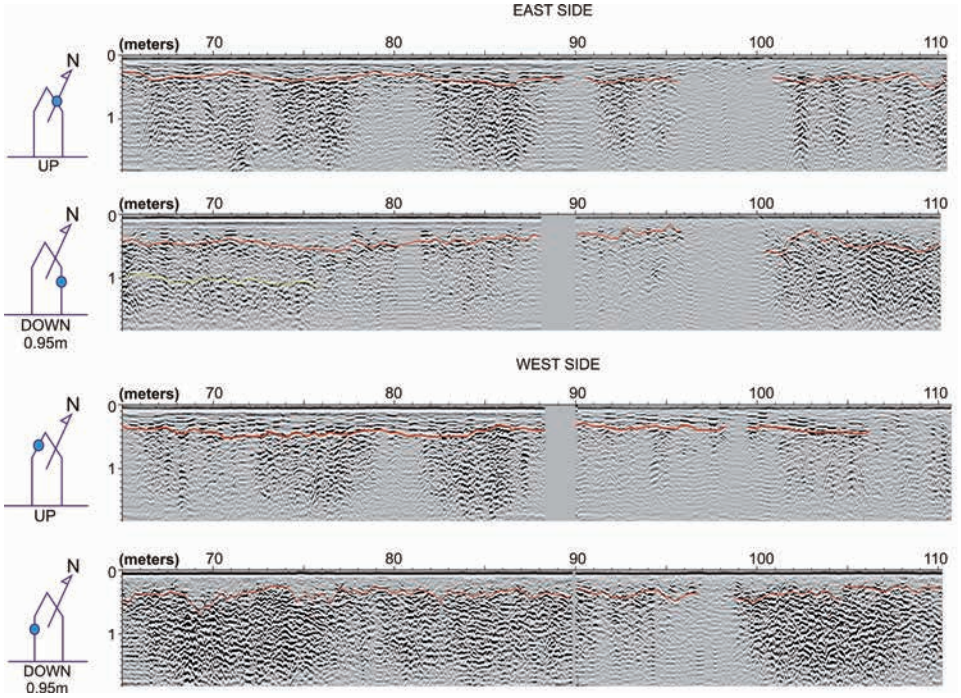

FIGURE 16
Processed GPR sections on the sidewalls of the archaic lining between the LDMS positions 0+65.0 m and 0+100.0 m. The small sketches on the left depict the direction of the profiles, whereas the dots mark the levels where they were carried out. Note that the first (from the top) and third profiles were conducted on the slabs forming the triangular arched roof.

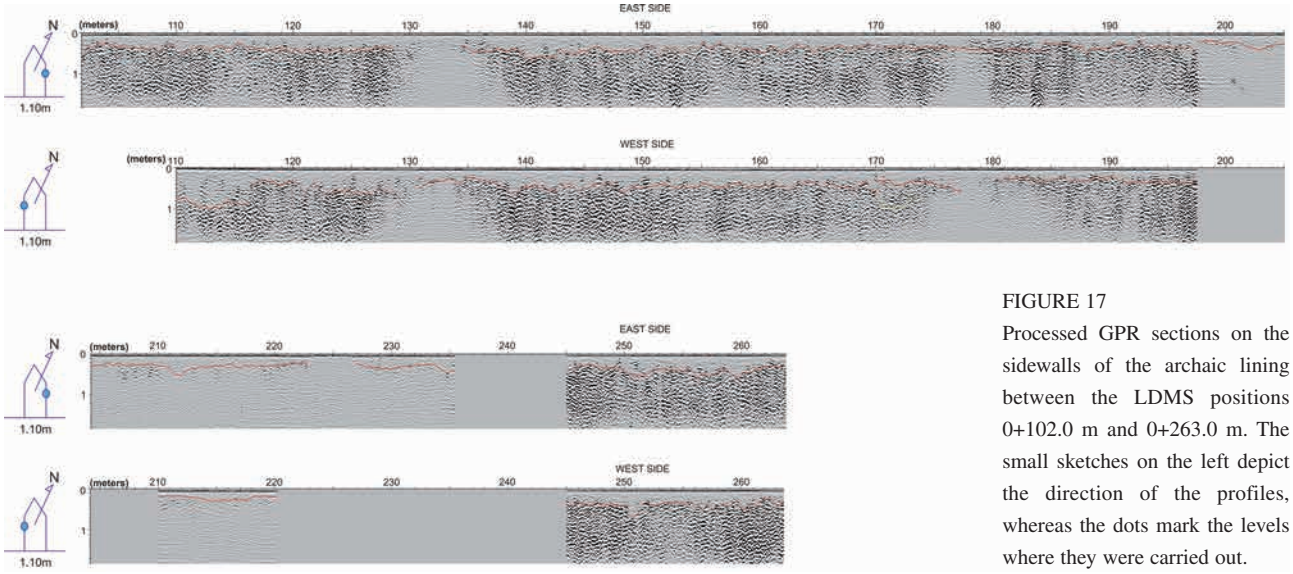

FIGURE 17
Processed GPR sections on the sidewalls of the archaic lining between the LDMS positions 0+102.0 m and 0+263.0 m. The small sketches on the left depict the direction of the profiles, whereas the dots mark the levels where they were carried out.

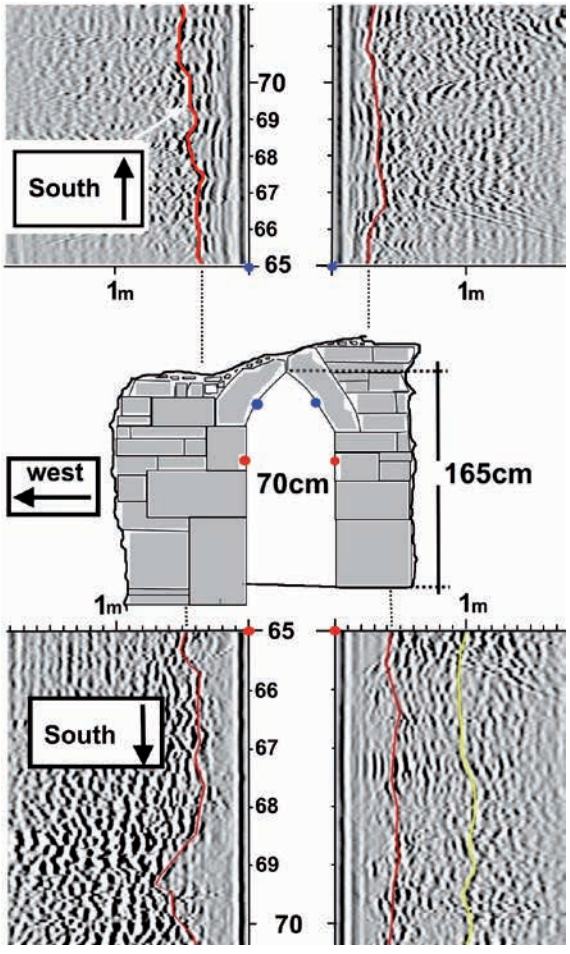

FIGURE 18
GPR results close to the point 0+63.0 m. Upper and lower images show the GPR results along the UP and DOWN profiles, respectively. The levels where the profiles took place are marked also by the red and blue points.

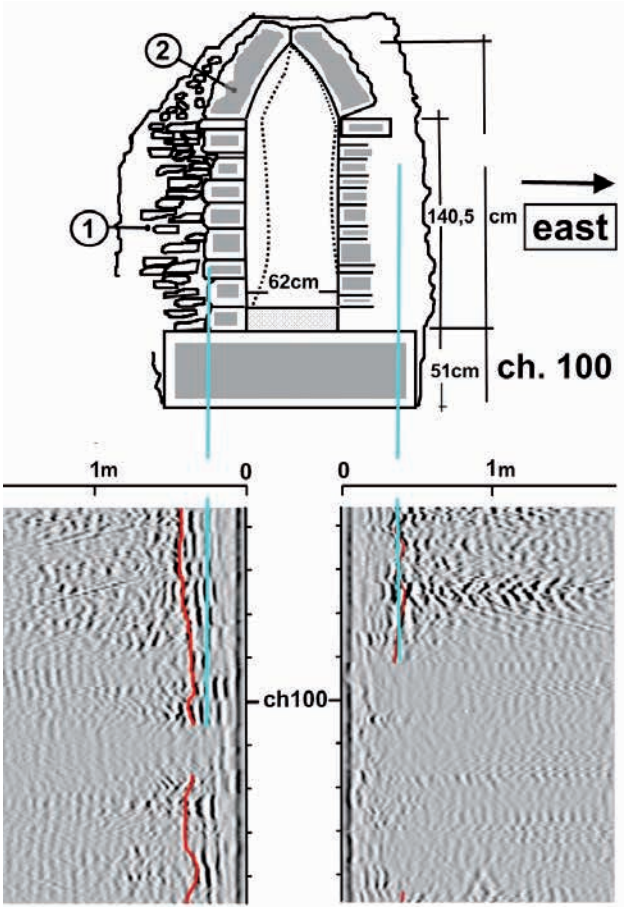

FIGURE 19
GPR results at the location 0+100.0 m. The red lines comprise the interpretation line that is attributed to the lining–backfill interface. The tunnel's cross section is a modified version of the drawing of Jantzen *et al.* (1973). 1: Well-structured backfill. 2: Hewn stones of the lining walls.

midpoint (CMP) arrangement to assess the velocity of the electromagnetic waves in the supporting walls. The move-out step was set at 0.10 m, and CMP profiles were conducted on the east and the west walls of the lining at the two ends of the tunnel both on the archaic and the Roman linings. The velocity analysis showed that the value of 0.09 m/nsec is the most representative one, and it was decided to use it throughout in our processing.

Figure 14 shows a member of the crew dragging the antennae to collect data along a profile on the archaic lining wall.

The archaic lining starts at the LDMS position 0+63.9 (Angistalis *et al*. 2014) while the portion between 0+10.0 m and 0+50.0 m was dressed in the Roman period. Four GPR profiles were carried out in this portion whose processed results are shown in Fig. 15 as depth sections. The profiles on the eastern sidewall were carried out at 1.3 m (UP) and 0.7 m (DOWN) above the floor, whereas those on the western one were carried out at the levels of 1.2 m and 0.7 m. As mentioned earlier, the velocity of the electromagnetic waves was set to 0.09 m/nsec. A clear continuous reflection (red line) is observed very close to the wall's surface at a distance varying about 0.3 m–0.5m. This is interpreted as being caused by the back side of the solid rock blocks of the lining's sidewalls. That is, this reflection corresponds to the interface between the lining's building stones and the backfill material.

The GPR signal disappears at some locations (example: east profile, DOWN, between the positions 10 and 15 of the LDMS), a fact that is interpreted as an influence of the increased moisture content at the particular spots. Another clue that supports this statement is the visible water dripping from the walls.

At some distance away from reflection of the back side of the lining, another one shows up rather clearly, though it is not present everywhere. This is attributed to the backfill–rock mass interface, which is undulating, proving several cave-in incidences during the initial drilling. According to the engineering terminology, a "cave-in incidence" is a collapse of the tunnel's roof due to the presence of poor ground, unfavourable orientation of rock discontinuities or faults, and/or excessive ground water pressure.

Clues similar as above can be inferred inspecting all the other GPR profiles. In fact, Figs 16 and 17 show results of the work done at the portions 65.0 m–110.0 m and 102.0 m–263.0 m. In every single one of the displayed profiles, the interface between the lining's wall and the backfill layer of partially worked stones is very well seen. The truth of our interpretation assumption can be checked at the point 0+63.9 where the archaic lining starts. A photograph of the lining elucidating its structure is included in Fig. 18, as well as radar sections for the first few meters of the profiles between 65.0 m and 110.0 m. The very good correspondence of the backside of the lining wall with the reflection appearing first in the sections is evident.

Note that the yellow line is a reflection that cannot be interpreted.

Figure 19 shows a comparison between the radar results and the structure of the tunnel at the location 0+100. Here, the west wall dismantled and reconstructed with brick mortared masonry

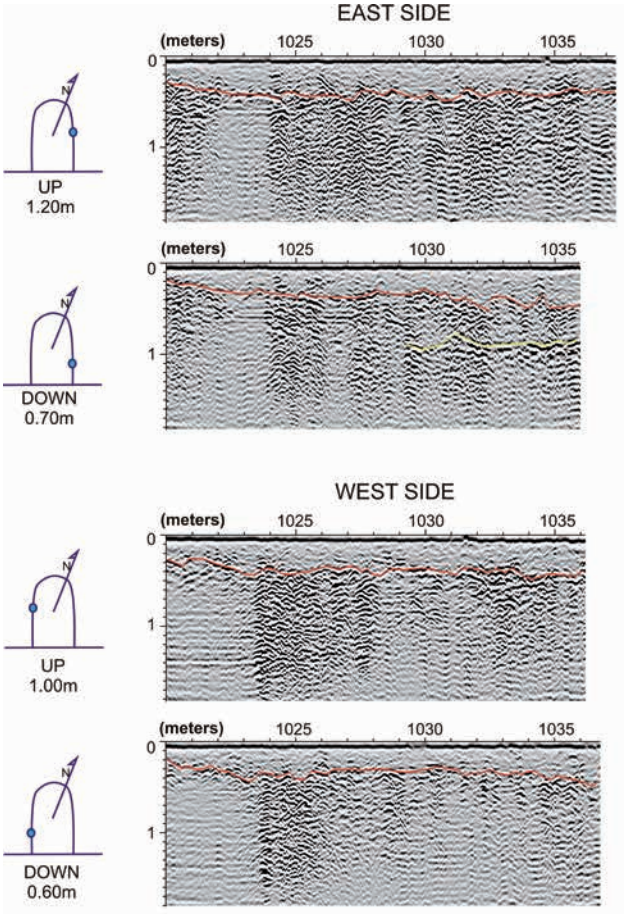

FIGURE 20
Processed GPR sections on the sidewalls of the Roman lining between the LDMS positions 0+1020.0 m and 0+1040.0 m. The small sketches on the left depict the direction of the profiles, whereas the dots mark the levels where they carried out.

by the archaeologists during the first investigation campaign (Jantzen *et al*. 1971). Thus the structure has been carefully drawn and is shown in our figure in a modified version after the study of Jantzen *et al*. (1971). The comparison of the reflection attributed to the back side of the lining wall with actual findings strengthens our interpretation.

Further, the profiles at the southern end, whose ground view is shown in Fig. 13, reveal also the width of the dressing wall (Fig. 20). However, another reflection that is further away from the surveying surface shows up. This is marked by a yellow line, and unfortunately no convincing interpretation has been offered so far.

CONCLUSIONS

ERT and GPR surveys were conducted on the surface of the supporting walls of the Eupalinian Tunnel at the island of Samos in Greece. Both showed their potential obtaining clues about the structure of the lining, the backfill area, and the original excavation.

The GPR method imaged the back side of the lining in great detail, and therefore, the width of this wall was assessed. On the other hand, ERT results mapped the ancient excavation front, behind the lining, and the backfilled area. The integrated results provided information that is considered of great importance for the design of the protection/restoration measures needed. Thus, the geophysical methods aided the overall effort to restore the tunnel and to render it accessible to the public.

ACKNOWLEDGEMENT

The authors are grateful to the company Egnatia Odos S.A. that financed this work, and they also thank architect Constantinos Zambas and Mrs. Maria Viglaki, director of the 21st Ephorate of Prehistoric and Classical Antiquities. They both provided invaluable information that was reclaimed for interpreting our results.

The second author appreciates the support of the Basic Research Project of Korea Institute of Geoscience and Mineral Resources.

REFERENCES

Angistalis G., Dounias G., Tsokas G.N. and Zambas K. 2014. Linings of Eupalinos Aqueduct, Samos Island, Greece. Description, Pathology and Proposed Restoration Measures. *Coastal Landscapes, Mining Activities, & Preservation of Cultural Heritage*, 17–20 September 2014, Milos Island, Greece.

Athanasiou E.N., Tsourlos P.I., Vargemezis G., Papazachos C.B. and Tsokas G.N. 2007. Non destructive DC resistivity surveying using flat-base electrodes. *Near Surface Geophysics* **5**(4), 243–272.

Apostol T.M. 2004. The Tunnel of Samos. *Engineering and Science* **1**, 30–40.

Burns A. 1971. The Tunnel of Eupalinus and the Tunnel Problem of Hero of Alexandria. *Isis* **62**(2), 172–185. JSTOR 229240.

Cosentino P. and Martorana R. 2001. The resistivity grid applied to wall structures: first results. *Proceedings of the 7th Meeting of the Environmental and Engineering Geophysical Society, European Section*, Birmingham, UK, ARCH02.

Colla C. and Maierhofer C. 2000. Investigation of historic masonry via radar reflection and tomography. In: *8th International Conference on Ground Penetrating Radar*, Gold Coast, Australia, 893–898.

Constable S., Parker R. and Constable C. 1991. Ocam's Inversion: a practical algorithm for generating smooth models from electromagnetic sounding data. *Geophysics* **52**, 289–300.

Dabas M., Stegeman C., Hesse A., Jolivet A., Mounir A. and Casas A. 1993. Prospection de la Cathedrale de Chartres. *Bull. Soc. Arch. d' Eure et Loir* **36**, 5–24.

Dabas M., Camerlynck C. and Freixas I Camps P. 2000. Simultaneous use of electrostatic quadrupole and GPR in urban context: investigation of the basement of the Cathedral of Girona (Catalunya, Spain). *Geophysics* **65**(2), 526–532.

Doerpfeld W. 1894. Die Ausgrabungen an der Enneakrunos. *Athenische Mitteilungen* **19**, 144–146.

Frumkin A. and Shimron A. 2006. Tunnel engineering in the Iron Age: Geoarchaeology of the Siloam Tunnel, Jerusalem. *Journal of Archaeological Science* **33**(2), 227–237.

Gaffney C. 2008. Detecting trends in the prediction of buried past: a review of geophysical techniques in archaeology. *Archaeometry* **50**(2), 313–336.

Goodfield J. and Toulmin S. 1965. How Was the Tunnel of Eupalinus Aligned? *Isis* **56**(1), 46–55. JSTOR 228457.

Guerin V. 1856. *Description de l'ile de Patmos et de l'ile de Samos*. August Durand, Libraire, Paris, pp. 328.

Grard R. and Taggagh A. 1991. A mobile four electrodes array and its application to electrical survey of planetary grounds at shallow depths. *Journal of Geophysical Research* **96**, 4117–4123.

Jantzen U., Felsch R.C.S., Hoepfner W. and Willers D. 1973. Samos 1971, AA 1973, 72 ff. Deutsche Archaeological Institute. Bericht I.

Kienast H.J. 1995. *Die Wasserleitung des Efpalinos auf Samos (Samos XIX.)*. Deutsches Archaologisches Institut, Bonn. Rudolph Habelt, ISBN 3-7749-2713-8, pp. 215.

Kienast H.J. 2005. *The Aqueduct of Eupalinos on Samos*. Greek Ministry of Culture Archaeological Receipts Fund, Athens, ISBN 960-214-424-6, pp.60.

Kuras O., Beamish D., Meldrun P.I. and Ogilvy R.D. 2006. Fundamentals of the capacitive resistivity technique. *Geophysics* **71**(3), G135–G152.

Leckebusch J. 2000. Two and three-dimensional ground penetrating radar surveys across a medieval choir: a case study in archaeology. *Archaeological Prospection* **7**, 189–200.

Linford N. 2004. From hypocauset to hyperbola: ground-penetrating radar surveys over mainly Roman remains in the U.K. *Archaeological Prospection* **11**, 237–246.

Mol L. and Preston P. 2010. The writing's in the wall: a review of new preliminary applications of electrical resistivity tomography within archaeology. *Archaeometry* **52**(6), 1079–1095.

Piro S., Goodman D. and Nishimura Y. 2003. The study and characterization of emperor Traiano's villa (Altopiani di Arcinazzo, Roma) using high-resolution integrated geophysical surveys. *Archaeological Prospection* **10**, 1–25.

Psilovikos A., Seitanidis G., Psilovikos A., Vavliakis E. and Margoni S. 2003. The Eypalinion tunnel in Samos: a water-supply construction with karst dynamics behaviour. *3rd Panhellenic Cave Symposium*, November 2003, Athens.

Sass O. and Viles H.A. 2006. How wet are these walls? Testing a novel technique for measuring moisture in ruined walls. *Journal of Cultural Heritage* **7**, 257–263.

Savvaidis A., Tsokas G.N., Liritzis Y. and Apostolou M. 1999. The location and mapping of ancient ruins on the castle of Lefkas (Greece) by resistivity and GPR methods. *Archaeological Prospection* **6**, 63–73.

Stamatakis M.G. 1990. Building stones from the ancient quarries of Agiades area, Samos Island, Greece. In: *The Engineering Geology Ancient Works, Monuments and Historical Sites (Preservation and Protection)*, Vol. 4 (eds P. Marinos P. and G. Koukis), pp. 2043–2047, Balkema, Rotterdam.

Stiros S.C. 2009. Orientation and alignment of the 5th century BC tunnel of Eupalinus at Samos (Greece). *Survey Review* **41**, 218–225.

Tabbagh A., Hesse A. and Grard R. 1993. Determination of electrical Properties of the ground at shallow depth with an electrostatic quadrupole: field trials on archaeological sites. *Geophysical Prospecting* **41**, 579–597.

Tsokas G.N., Stampolidis A., Mertzanidis I., Tsourlos P.I., Hamza R., Chrisafis C. *et al*. 2007. Geophysical exploration in the church of Protaton in Karyes of Mount Athos (Holy Mountain) in Northern Greece. *Archaeological Prospection* **14**, 75–86.

Tsokas G.N., Tsourlos P.I., Vargemezis G. and Novack M. 2008. Non destructive ERT for indoors investigations: the case of Kapnikarea Church in Athens. *Archaeological Prospection* **15**, 47–61.

Tsokas G.N., Tsourlos P.I., Kim J.-H., Papazachos C.B., Vargemezis G. and Bogiatzis P. 2014. Assessing the condition of the rock mass over the tunnel of Eupalinus in Samos (Greece) using both conventional geophysical methods and surface to tunnel ERT. *Archaeological Prospection* (in press).

Tsourlos P.I. 1995. *Modelling, interpretation and inversion of multielectrode resistivity survey data*. PhD thesis, University of York, U.K.

Tsourlos P.I. and Tsokas G.N. 2007. Archaeological prospection by means of fully non destructive DC resistivity surveying. Studijne zvesti archeologickeho ustvu sav. *Archaeological Prospection* **41**, 252–254.

Tsourlos P.I. and Tsokas G.N. 2011. Non-destructive Electrical Resistivity Tomography Survey at the South Walls of the Acropolis of Athens. *Archaeological Prospection* **18**, 173–186.

Van der Waerden B.L. 1968. Eupalinos and His Tunnel. *Isis* **59**(1), 82–83. JSTOR 227855.

Viles H., Sass O. and Mol L. 2008. 2D Resistivity surveys as a tool for investigating moisture In historic masonry walls. *SMW08 International workshop "In situ monitoring of monumental Surfaces"*, Florence, Italy, 27–29 October 2008, 91–96.

Zambas K. 2009. Final study for the restoration, final architectonical study for shaping and implementation study of the Eupalinian Tunnel in Samos. Greek Ministry of Culture: KE N5400-4180-B-R-D-1-A-EE1, (in Greek).